

# Reactions of Laser-Ablated Nickel Atoms with Dioxygen. Infrared Spectra and Density Functional Calculations of Nickel Oxides NiO, ONiO, Ni<sub>2</sub>O<sub>2</sub>, and Ni<sub>2</sub>O<sub>3</sub>, Superoxide NiOO, Peroxide Ni(O<sub>2</sub>), and Higher Complexes in Solid Argon

Angelo Citra, George V. Chertihin, and Lester Andrews\*

Department of Chemistry, University of Virginia, Charlottesville, Virginia 22901

Matthew Neurock

Department of Chemical Engineering, University of Virginia, Charlottesville, Virginia 22901

Received: December 17, 1996; In Final Form: February 26, 1997<sup>⊗</sup>

Laser-ablated nickel atoms react with dioxygen to form the primary oxides NiO and ONiO, some of which combine to form the secondary oxides Ni<sub>2</sub>O<sub>2</sub> and ONiONiO during condensation in excess argon at 10 K. The insertion product dioxide ONiO is linear based on natural nickel and <sup>18</sup>O isotopic substitution and DFT calculations. Annealing produces the cyclic adducts reported in earlier thermal nickel experiments and the new NiOO superoxide species, which are characterized by isotopic shifts and DFT structure and frequency calculations. In addition, dioxygen complexes with NiO and ONiO were also observed. Finally, the matrix provides sharp bands and the resolution to observe nickel isotopic splittings which characterize the Fermi-resonance interaction in the ONiOO and (O<sub>2</sub>)Ni(O<sub>2</sub>) molecules.

## Introduction

Recent matrix infrared investigations of laser-ablated iron atom + oxygen molecule reactions revealed three primary product structural isomers: bent FeOO, bent OFeO, and cyclic Fe(O<sub>2</sub>). Complementary DFT calculations confirmed these spectroscopic assignments and identified the ground electronic states by comparison of observed and DFT calculated isotopic frequencies.<sup>1,2</sup> Nickel is also an important metal in materials and chemistry, and the characterization of different nickel oxide structures is of interest. Since laser-ablated metal atoms contain excess energy<sup>3</sup> and undergo reactions that require activation energy, the new ONiO oxidative insertion product is expected. However, with two additional d-electrons, a linear structure is predicted for the ONiO nickel dioxide molecule.<sup>4</sup> Previous nickel oxide results are available only for the NiO diatomic molecule, which was observed first in solid argon<sup>5</sup> and then in the gas phase<sup>6,7</sup> and characterized by several theoretical calculations.<sup>8–10</sup>

The reaction of thermal Ni atoms with O<sub>2</sub> was reported by Ozin and co-workers over 20 years ago.<sup>11</sup> Two products were observed and characterized as cyclic Ni(O<sub>2</sub>) and bicyclic (O<sub>2</sub>)-Ni(O<sub>2</sub>) with a D<sub>2d</sub> structure. An asymmetric addition product NiOO was not reported, but the recent characterization of FeOO in this laboratory<sup>1,2</sup> suggests that an analogous NiOO molecule should be observable. We describe here a complementary study of laser-ablated Ni reactions with O<sub>2</sub> and DFT calculations of product molecule structures, electronic states, and isotopic frequencies.

## Experimental Section

The technique for laser ablation and FTIR matrix investigation was identical to that employed previously for the iron–oxygen system.<sup>1,2</sup> Nickel (Johnson-Matthey, 99.99%) was used for the laser target. Oxygen samples (Matheson, Yeda 55% and 99% <sup>18</sup>O) were used as received. Typical matrix dilution was 0.2–1% in argon and nitrogen (Matheson). Gas mixtures were

codeposited 1–2 h on a 10 ± 1 K CsI window at 2–6 mmol/h with ablated Ni atoms using 10–40 mJ pulses of 1064 nm radiation from a Nd:YAG laser. Annealing and photolysis by a medium-pressure mercury arc (Philips, 175 W) with globe removed were also done. FTIR spectra were recorded with 0.5 cm<sup>-1</sup> resolution on a Nicolet 750 spectrometer.

## Results

FTIR spectra of the Ni + O<sub>2</sub> system in solid Ar and N<sub>2</sub> will be presented.

**Ni + O<sub>2</sub>/Ar.** The relative infrared intensities of product bands in the Ni + O<sub>2</sub> system depended strongly on laser power and oxygen concentration. Argon blank experiments revealed two very weak doublets at 954.9/949.3 and 825.7/822.8 cm<sup>-1</sup> with intensity distributions 2.5:1.0, which are in good agreement with natural isotopic nickel (major isotopes <sup>58</sup>Ni, 67.9%, and <sup>60</sup>Ni, 26.2%). Increasing oxygen concentration increased these bands and produced a weak 967.1 cm<sup>-1</sup> band. Spectra are shown in Figure 1 for 1% O<sub>2</sub>. The latter doublet is in agreement (±0.1 cm<sup>-1</sup>) with that assigned to the NiO molecule in solid argon.<sup>5</sup> It is interesting to note that the relative intensities of many bands listed in Table 1 depended on whether these first two doublets were strong or weak, which clearly indicates that the above doublets are the first reaction products. Six bands at 1498.9 (broad, not shown), 1393.7, 1221.3, 1135.8, 1095.5, and 1063.9 cm<sup>-1</sup> grew on annealing (Figures 1 and 2). The first four bands were not observed on deposition but appeared as weak bands on annealing; the last two bands were weak in the spectra after deposition in experiments with higher oxygen concentration and higher laser power but grew into strong bands on annealing, and the latter band gave a clear nickel isotopic splitting at 1062.6 cm<sup>-1</sup>. The relative intensities of product bands dramatically changed in the 1000–900 cm<sup>-1</sup> region with increasing oxygen concentration. Very strong bands were observed at 973.9 and 967.1 cm<sup>-1</sup> after annealing. The latter band was detected on deposition while the former band appeared in the spectra only after annealing and showed Ni isotopic structure 973.9/972.4/970.8 cm<sup>-1</sup>. Here we must note that the

<sup>⊗</sup> Abstract published in *Advance ACS Abstracts*, April 1, 1997.

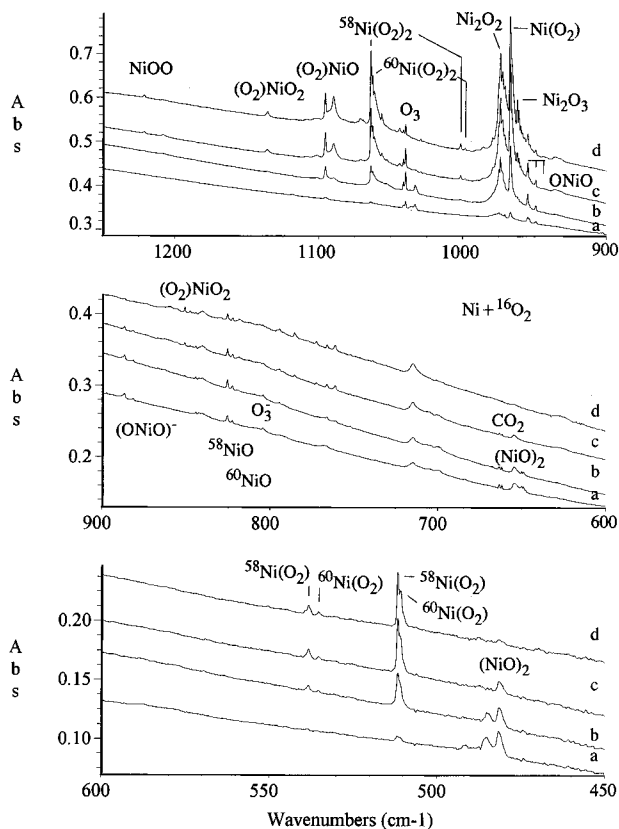


**Figure 1.** Infrared spectra in the 1250–450  $\text{cm}^{-1}$  region for laser-ablated Ni atoms reacting with 1%  $\text{O}_2$  in argon during condensation at 10 K: (a) 2 h deposition, (b) after annealing to 20 K, (c) after annealing to 30 K, and (d) after annealing to 40 K.

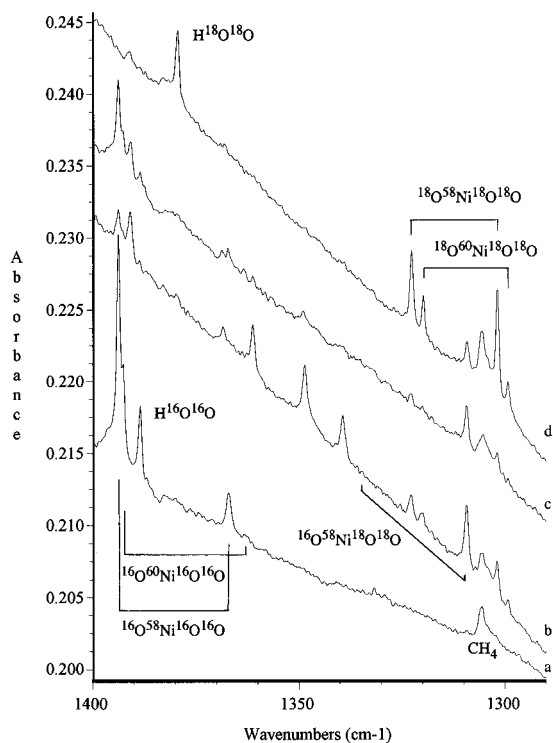


**Figure 2.** Infrared spectra in the 1400–1300  $\text{cm}^{-1}$  region for laser-ablated Ni atoms reacting with isotopic oxygen samples in argon shown after 30 K annealing to enhance the new product absorption: (a) 0.5%  $^{16}\text{O}_2$ , (b) 1%  $^{16,18}\text{O}_2$  ( $^{16}\text{O}_2 + ^{16}\text{O}^{18}\text{O} + ^{18}\text{O}_2$ ), (c) 1%  $^{16}\text{O}_2 + 0.5\%$   $^{18}\text{O}_2$ , and (d) 0.5%  $^{18}\text{O}_2$ . Absorbance scale is for spectrum (a).

977 and 972  $\text{cm}^{-1}$  bands previously assigned to the  $\text{N}_2\text{Ni}(\text{O}_2)$  and  $(\text{N}_2)_2\text{Ni}(\text{O}_2)$  molecules<sup>11</sup> are very close to the new 973.9

$\text{cm}^{-1}$  band in the present work. In the high-frequency region, a very weak 2089.4  $\text{cm}^{-1}$  band ( $A = 0.01$ ) was detected<sup>12</sup> for NiNN, and annealing produced a weak 2243.4  $\text{cm}^{-1}$  band ( $A = 0.05$ ) for NNNi( $\text{O}_2$ ) and weaker 2283.4, 2260.5  $\text{cm}^{-1}$  bands ( $A = 0.01$ ) for  $(\text{NN})_2\text{Ni}(\text{O}_2)$ ;<sup>13</sup> even though trace  $\text{N}_2$  is present,  $\text{N}_2$  complexes make only a minor contribution to the present 974  $\text{cm}^{-1}$  band system. Special experiments with  $\text{O}_2/\text{N}_2/\text{Ar}$  mixtures revealed broad bands with maxima at 979.2 and 976.4  $\text{cm}^{-1}$ , which are clearly different, and produced markedly increased bands in the 2000  $\text{cm}^{-1}$  region, in agreement with previous workers.<sup>12</sup>

The 900–700  $\text{cm}^{-1}$  region revealed several weak absorptions, and the NiO doublet was the strongest among them. These bands were weak especially in experiments with isotopic mixtures, and many experiments with different laser power and oxygen concentration were done to detect isotopic counterparts. New doublets at 886.8/881.6 and 844.6/842.6  $\text{cm}^{-1}$  in the spectra after deposition with high laser power decreased on annealing; these doublets were stronger when the 954.9/949.3  $\text{cm}^{-1}$  and NiO doublet were stronger, respectively. Weak 851.1, 848.0  $\text{cm}^{-1}$  and 766.1, 762.4  $\text{cm}^{-1}$  doublets appeared on annealing (Figure 1d). Below 700  $\text{cm}^{-1}$  four main bands 654.2, 538.3/535.3, 511.7/510.9, and 481.6  $\text{cm}^{-1}$  were observed. The two 2.5:1 doublets behaved similarly to the 967.1  $\text{cm}^{-1}$  band on annealing. The first and the last bands appeared in the spectra after deposition and decreased after annealing and again were stronger when the 954.9/949.3  $\text{cm}^{-1}$  and NiO bands were stronger.

Several samples were subjected to broad-band photolysis. Photolysis immediately after deposition destroyed the 1393.7  $\text{cm}^{-1}$  band, halved the 654.2, 481.6, 485.1  $\text{cm}^{-1}$  bands, and slightly decreased the 1095.5  $\text{cm}^{-1}$  band. Photolysis after annealing almost destroyed the 1221.3, 1135.8, and 851.0  $\text{cm}^{-1}$  bands and had the same effect on the above bands. Further annealing regenerated these bands, and further photolysis again had the same effect.

Oxygen isotopic substitution was employed for band identification and assignment, band positions are listed in Table 1, and spectra for isotopic mixtures are shown in Figures 2, 3, and 4. The 1393.7  $\text{cm}^{-1}$  band gave two pure oxygen-18 counterparts with clear nickel isotopic splittings! The 1221.3  $\text{cm}^{-1}$  band shifted to 1153.2  $\text{cm}^{-1}$  with  $^{18}\text{O}_2$  and produced three bands with the statistical mixture ( $^{16}\text{O}_2\text{:}^{16}\text{O}^{18}\text{O}\text{:}^{18}\text{O}_2 = 1\text{:}2\text{:}1$ ), but the broader middle component was partially resolved. The 1135.8  $\text{cm}^{-1}$  band gave a broad triplet. The 1095.5  $\text{cm}^{-1}$  band produced sharp triplet and doublet absorptions with statistical and mechanical ( $^{16}\text{O}_2\text{:}^{18}\text{O}_2 = 1\text{:}1$ ) mixtures, respectively. The 1063.9  $\text{cm}^{-1}$  absorption produced eight counterpart bands in experiments with the statistical mixture, and six of these exhibited resolved nickel isotopic splittings.

Isotopic structures in the 1000–900  $\text{cm}^{-1}$  region overlapped, but the 967.1 and 954.9/949.3  $\text{cm}^{-1}$  bands produced triplets with the statistical mixture and doublets with the mechanical mixture. The 973.9  $\text{cm}^{-1}$  band gave a mixed isotopic quartet. The 886.8/881.6, 844.6/842.6, and 825.6/822.5  $\text{cm}^{-1}$  bands produced triplet, doublet, and doublet absorptions, respectively, in experiments with statistical isotopic oxygen.

An unusual pattern was observed for the 654.2  $\text{cm}^{-1}$  band. In experiments with the statistical isotopic mixture, a 1:1:1:1 quartet with one higher and one intermediate component was found, but only pure isotopic components were observed with the mechanical mixture. Other bands in this region produced triplets and doublets in experiments with statistical and me-

**TABLE 1: Infrared Absorptions (cm<sup>-1</sup>) Observed for the Laser-Ablated Ni + O<sub>2</sub> Reaction Products Isolated in Solid Argon**

<sup>16</sup> O <sub>2</sub>	<sup>18</sup> O <sub>2</sub>	<sup>16</sup> O <sub>2</sub> + <sup>16</sup> O <sup>18</sup> O + <sup>18</sup> O <sub>2</sub>	anneal	16/18	assignt
1498.9	1414.6	1499, 1462, 1458, 1415	+	1.0596	(X)OO
1393.7	1322.7	1393.7, 1391.0, 1368.5, 1361.2	+	(1.06)	O <sup>58</sup> NiOO
1367.1	1301.8	1348.6, 1339.4, 1335.3, 1322.7 1309.3, 1301.8			
1392.7, 1363.2	1319.9, 1299.3		+		O <sup>60</sup> NiOO
1221.3	1153.2	1221.1, 1188.0, 1187.8, 1153.9	++	1.0591	NiOO
1135.8	1073.1	1035.8, 1104.9, 1073	++	1.0584	(O <sub>2</sub> )NiO <sub>2</sub>
1095.5	1034.6	1095.5, 1065.6, 1034.6	++	1.0589	(O <sub>2</sub> )NiO
1089.8	1030.6	1089.8, 1030 sh	++	1.0575	site
1063.9	1009.9	1063.9, 1046.2, 1036.6, 1082.2, 1078.1, 1009.9	++	1.0535	(O <sub>2</sub> ) <sup>58</sup> Ni(O <sub>2</sub> ) ν(O—O) B <sub>u</sub>
1062.6	1007.7	1062.6, 1044.5 1081.5, 1077.3, 1007.7	++	1.0545	(O <sub>2</sub> ) <sup>60</sup> Ni(O <sub>2</sub> )
1061.4	1006.2		+	1.0548	site
1001.4	955.8	1019.1, 1002.6		1.0471	(O <sub>2</sub> ) <sup>50</sup> Ni(O <sub>2</sub> ) ν(sum)
998.2	953.2	1016.7	+	1.0472	(O <sub>2</sub> ) <sup>60</sup> Ni(O <sub>2</sub> ) ν(sum)
973.9	928.9	973.6, 972.4, 931.3, 929.0	+	1.0484	<sup>58</sup> NiO <sup>58</sup> NiO
972.4	927.8, 927.2	931.4, 930.4, 929.1	+	1.0484	<sup>58,60</sup> Ni <sub>2</sub> O <sub>2</sub>
970.8	926.2	928, 927.4	+	1.0482	<sup>60</sup> NiO <sup>60</sup> NiO
967.1	914.5	967.1, 941.3, 914.5	+	1.0575	Ni(O <sub>2</sub> )(ν <sub>1</sub> )
962.3	917.1	962.3, 961.1, 922.4, 920.7, 917.1	+	1.0493	O <sup>58</sup> NiO <sup>58</sup> NiO
961.1	915.8		+	1.0495	O <sup>58</sup> NiO <sup>60</sup> NiO
959.9	masked		+	1.0495	O <sup>60</sup> NiO <sup>60</sup> NiO
953.7	901.7	sextet	—	1.0577	O <sub>4</sub> <sup>-</sup>
954.9	920.5	954.9, 939.5, 920.5	+—	1.0377	O <sup>58</sup> NiO(ν <sub>3</sub> )
949.3	masked		+—		O <sup>60</sup> NiO(ν <sub>3</sub> )
944.1			+—		O <sup>62</sup> NiO(ν <sub>3</sub> )
951.5	909.6		+	1.0461	( <sup>58</sup> Ni <sub>2</sub> O <sub>3</sub> )(X) ( <sup>58</sup> Ni <sup>60</sup> NiO <sub>3</sub> )(X)
950.1			+		
886.8	854.8	886.8, 872.8, 854.8	—	1.0374	(O <sup>58</sup> NiO) <sup>-</sup>
881.6	849.4		—	1.0379	(O <sup>60</sup> NiO) <sup>-</sup>
851.0	816.3		+	1.0425	(O <sub>2</sub> ) <sup>58</sup> NiO <sub>2</sub>
848.0	812.5		+	1.0437	(O <sub>2</sub> ) <sup>60</sup> NiO <sub>2</sub>
844.6	804.6	844.6, 804.6	—	1.0497	(Ni <sup>58</sup> NiO)
842.6	802.7	842.6, 802.7	—	1.0497	(Ni <sup>60</sup> NiO)
825.7	789.4	825.7, 789.4	—	1.0460	<sup>58</sup> NiO
822.8	786.3	822.8, 786.3	—	1.0464	<sup>60</sup> NiO
820.2			—		<sup>62</sup> NiO
804.5	759.2	sextet	—	1.0597	O <sub>3</sub> <sup>-</sup>
795, 786	751, 742		+	1.059	Ni <sup>+</sup> O <sub>3</sub> <sup>-</sup>
766.1	737.8	?	+	1.0384	( <sup>58</sup> NiO <sub>x</sub> )?
	734.0	?	+		( <sup>60</sup> NiO <sub>x</sub> )?
654.2	625.5	676.2, 654.2, 632.8, 625.5	—	1.0459	(Ni <sub>2</sub> O <sub>2</sub> ) site
650.2	621.7	650.2, 626.4, 621.7	—	1.0458	( <sup>58</sup> Ni <sup>58</sup> NiO <sub>2</sub> )
649.0	620.5	625.4	—	1.0459	( <sup>58</sup> Ni <sup>60</sup> NiO <sub>2</sub> )
648.0	619.4		—	1.0461	( <sup>60</sup> Ni <sup>60</sup> NiO <sub>2</sub> )
614.4	587.1	614.4, 596.5, 587.1	+	1.0465	( <sup>58</sup> Ni <sup>58</sup> NiO <sub>2</sub> )O
613.3	586.0	595.5	+	1.0466	( <sup>58</sup> Ni <sup>60</sup> NiO <sub>2</sub> )O
612.4	585.1	594.3	+	1.0467	( <sup>60</sup> Ni <sup>60</sup> NiO <sub>2</sub> )O
538.3	518.8	538.3, 530.2, 518.8	+	1.0374	<sup>58</sup> Ni(O <sub>2</sub> )(ν <sub>2</sub> )
535.3	516.1		+	1.0372	<sup>60</sup> Ni(O <sub>2</sub> )(ν <sub>2</sub> )
511.7	485.7	511.7, 496.3, 480.7	+	1.0535	<sup>58</sup> Ni(O <sub>2</sub> )(ν <sub>3</sub> )
510.9	484.8	510.9, 495.4, 484.8	+	1.0538	<sup>60</sup> Ni(O <sub>2</sub> )(ν <sub>3</sub> )
485.1	463.9	485.1, 475.4, 463.9	—	1.0468	(NiO) <sub>2</sub> site
481.6	460.1	481.6, 471, 460.1	—	1.0467	(NiO) <sub>2</sub>

chanical mixtures, respectively. Details of isotopic substitution will be discussed with band assignments.

**Ni + N<sub>2</sub>O/Ar.** A similar experiment with the N<sub>2</sub>O reagent gave different product populations. First, the 825.7/822.8 cm<sup>-1</sup> doublet was 4 times stronger and exhibited a weaker component at 820.2 cm<sup>-1</sup> whereas the 954.9/949.3 cm<sup>-1</sup> doublet was only one-fifth as strong as in Figure 1a. The 1095.5 cm<sup>-1</sup> band was one-half as strong with N<sub>2</sub>O and after annealing was 4 times stronger than the 1063.9 cm<sup>-1</sup> band. The 1393.7 cm<sup>-1</sup> band was weak in the deposited sample and increased markedly on annealing. A weak resolved 974.8/973.3/971.9 cm<sup>-1</sup> triplet dominated the 900 cm<sup>-1</sup> region; annealing produced a weak 962.6/961.4/960.2 cm<sup>-1</sup> triplet and a very weak 967.1 cm<sup>-1</sup> band. Although the 825.7/822.8 cm<sup>-1</sup> doublet was 4 times stronger with N<sub>2</sub>O, the 654 and 482 cm<sup>-1</sup> bands were only half as strong.

**Ni + O<sub>2</sub>/N<sub>2</sub>.** Reaction of iron atoms with oxygen led to formation of different products in Ar and N<sub>2</sub> matrices.<sup>2,14</sup> The nickel–oxygen system was also investigated in nitrogen matrices in order to explore this difference. In the 1000–900 cm<sup>-1</sup> region the main product bands after deposition were 990.7 (O<sub>4</sub><sup>-</sup>), 970.1, and 959.5/953.9 cm<sup>-1</sup>, which decreased on annealing. Weaker doublets were observed at 894.4/889.2, 849.5/847.5, and 760.5/758.1 cm<sup>-1</sup>, which also decreased on annealing. These bands shifted to 936.3 cm<sup>-1</sup> (<sup>18</sup>O<sub>4</sub><sup>-</sup>) and 919.0, 924.8/921.3, 862.2/856.8, 809.4/807.1, and 726.3 cm<sup>-1</sup> with <sup>18</sup>O<sub>2</sub>. Traces of NO and (NO)<sub>2</sub> were also observed along with a sharp weak 1749.6 cm<sup>-1</sup> band with oxygen-18 counterpart at 1713.5 cm<sup>-1</sup>.

### Calculations

All-electron DFT calculations were done using the DGauss program developed by Cray Research,<sup>15</sup> which employs opti-

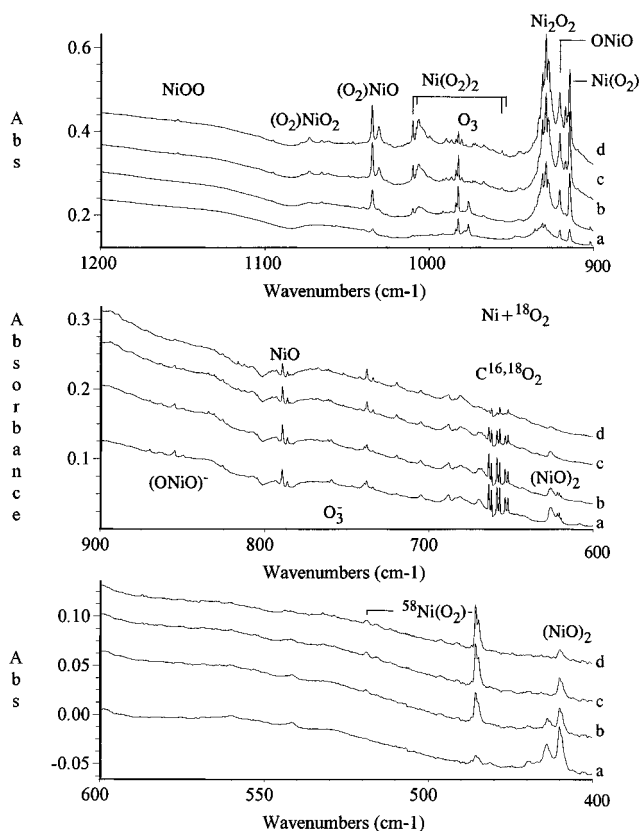


**Figure 3.** Infrared spectra in the 1200–450  $\text{cm}^{-1}$  region for laser-ablated Ni atoms reacting with 0.5%  $^{18}\text{O}_2$  in argon during condensation at 10 K: (a) 3 h deposition, (b) after annealing to 20 K, (c) after annealing to 30 K, and (d) after annealing to 40 K.

mized Gaussian basis functions to self-consistently solve the single-particle Kohn–Sham equations.<sup>16</sup> The local spin-density exchange–correlation potentials represented by Vosko–Wilk–Nusair potential<sup>17</sup> while nonlocal gradient corrections to the exchange and correlation are determined in-situ to SCF calculation via exchange and correlation Becke and Perdew potentials, respectively.<sup>18–20</sup> SCF convergence reported here was  $1 \times 10^{-6}$  au for energy and  $1 \times 10^{-3}$  au/Å for structural optimization. Second derivatives, force constants, and frequencies were determined numerically in the harmonic oscillator approximation. DFT-optimized DZVP quality basis sets were used for both nickel (963321/531/41) and oxygen (621/41/1).<sup>21</sup>

The NiO, NiO<sub>2</sub>, NiO<sub>3</sub>, NiO<sub>4</sub>, and Ni<sub>2</sub>O<sub>2</sub> molecules were calculated, and the results are summarized in Tables 2–5. DFT calculations found that the ground state of NiO is a triplet with frequency 823  $\text{cm}^{-1}$ , which is in good agreement with the matrix experiments and previous work.<sup>5,6,10</sup> The calculated bond length, 1.644 Å, is in excellent agreement with the recently measured 1.627 Å value.<sup>7</sup> The singlet state of linear ONiO was found to be more stable by 8 kcal/mol than the triplet state, and the latter had an imaginary bending frequency. For Ni(O<sub>2</sub>) and NiOO all states are higher energy than the singlet ONiO state; singlet, triplet, and quintet Ni(O<sub>2</sub>) are higher by 20, 17, and 52 kcal/mol, respectively, and have distinctly different Ni–O<sub>2</sub> modes (Table 2). Singlet NiOO is higher by 34 kcal/mol, and higher spin states converged to the cyclic isomer. Three NiO<sub>3</sub> isomers were found, which are presented in Table 3. For the ONi(O<sub>2</sub>) isomer ( $C_{2v}$ ) the ground state is triplet, and singlet and quintet states are 11 and 16 kcal/mol higher. The bent singlet ONiOO isomer is 10 kcal/mol higher, but the triplet  $D_{3h}$  isomer is 21 kcal/mol higher than the triplet state of ONi(O<sub>2</sub>). Several isomers with different multiplicities were found for NiO<sub>4</sub> molecules. The lowest among them are planar  $C_{2h}$  (almost  $D_{2h}$ )

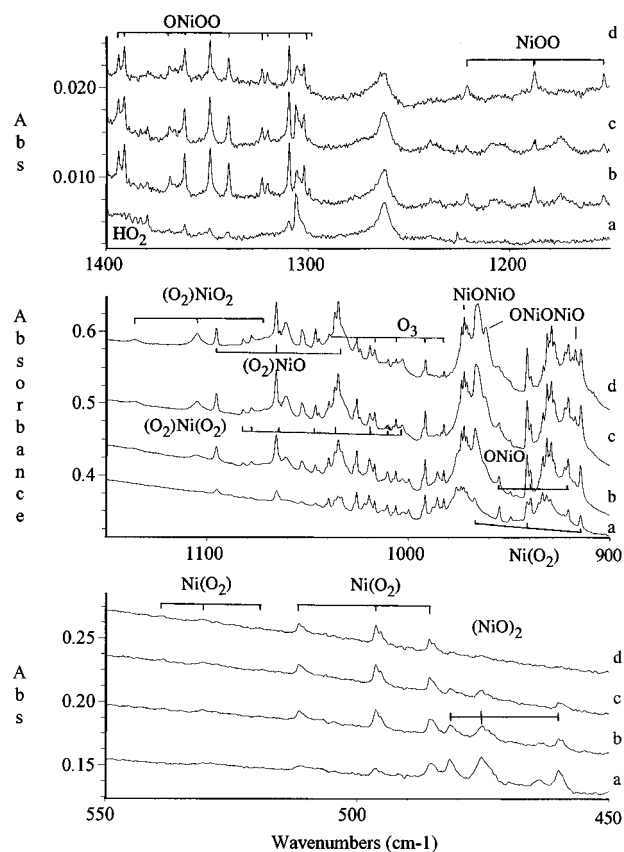


**Figure 4.** Infrared spectra in the 1400–450  $\text{cm}^{-1}$  region for laser-ablated Ni atoms reacting with 1%  $^{16}\text{O}_2 + ^{16}\text{O}^{18}\text{O} + ^{18}\text{O}_2$  in argon during condensation at 10 K: (a) 2 h deposition, (b) after annealing to 20 K, (c) after annealing to 30 K, and (d) after annealing to 40 K.

triplet and singlet (6 kcal/mol higher). The triplets (O<sub>2</sub>)NiOO and O<sub>2</sub>Ni(O<sub>2</sub>) are 21 and 68 kcal/mol higher, respectively, than the triplet  $C_{2h}$  structure. The highest isomer (+100 kcal/mol) is the tetrahedral molecule. Table 4 contains results for the (O<sub>2</sub>)Ni(O<sub>2</sub>), (O<sub>2</sub>)NiOO, and (O<sub>2</sub>)NiO<sub>2</sub> molecules. For rhombic Ni<sub>2</sub>O<sub>2</sub> singlet and triplet states with energy difference 0.2 kcal/mol were found (Table 5). Finally, Figure 5 diagrams the DFT optimized structures for the product molecules observed here.

## Discussion

Assignment of spectral bands will be presented for each molecule in turn.

**NiO.** The sharp bands in argon matrices at 825.7 and 822.8  $\text{cm}^{-1}$  are assigned to the NiO molecule. The oxygen 16/18 isotopic ratio 1.0460 is just below the harmonic value 1.0466. The intensity distribution 2.5:1.0 is appropriate for nickel isotopes in natural abundance; the nickel 58/60 ratio 1.003 52 is also slightly lower than the harmonic value 1.003 63. These results are in an excellent agreement with previous work where a 825.74/822.88  $\text{cm}^{-1}$  doublet was assigned to the  $^{58}\text{NiO}$  and  $^{60}\text{NiO}$  molecules.<sup>5</sup> In a high yield NiO experiment, the  $^{62}\text{NiO}$  band was observed here at 820.2  $\text{cm}^{-1}$ . The DFT calculated frequency 823  $\text{cm}^{-1}$  also agrees with experiment and previous calculations.<sup>8–10</sup>

The matrix  $^{58}\text{Ni}^{16}\text{O}$  fundamental, 825.7  $\text{cm}^{-1}$ , is 2.6  $\text{cm}^{-1}$  red-shifted from the recently determined 828.3  $\text{cm}^{-1}$  gas phase value.<sup>6</sup> The FeO molecule is, however, blue-shifted 1.5  $\text{cm}^{-1}$  by the argon matrix.<sup>2</sup> The formation of NiO is taking place on the matrix surface during deposition by reaction 1.



**TABLE 2: DFT Calculated Geometry, Frequencies (cm<sup>-1</sup>), and Intensities (km/mol) for NiO and NiO<sub>2</sub> Isomers**

molecule	R(Ni-O), R(O-O), Å	angle, deg	$\nu_1$ (I)	$\nu_2$ (I)	$\nu_3$ (I)
NiO triplet	1.644		823 (43) 786 (39) <sup>a</sup>		
ONiO singlet <sup>b</sup>	1.613	180	805 (0) 758 (0) <sup>a</sup>	48 (12) 47 (11)	1027 (63) 989 (58)
Ni(O <sub>2</sub> ) singlet <sup>c</sup>	1.792	46 (ONiO)	1029.4 (22) 972.0 (20) <sup>a</sup>	599.2 (3) 576.4 (3)	477.8 (16) 453.0 (15)
Ni(O <sub>2</sub> ) triplet <sup>c</sup>	1.844	44 (ONiO)	1037 (82) 979 (73) <sup>a</sup>	516 (0) 497 (0)	60 (41) 56 (37)
NiOO singlet <sup>c</sup>	1.721 1.302	123 (NiOO)	1227 (295) 1157 (261) <sup>a</sup>	265 (10) 252 (9)	622 (13) 595 (11)

<sup>a</sup> The second frequency and intensity are given for <sup>18</sup>O-enriched isotopic molecule. <sup>b</sup> Triplet ONiO is 8 kcal/mol higher. <sup>c</sup> Singlet, triplet Ni(O<sub>2</sub>) and singlet NiOO are higher by 20, 17, and 34 kcal/mol, respectively, than singlet ONiO.

**TABLE 3: DFT Calculated Frequencies (cm<sup>-1</sup>) and Intensities (km/mol) for NiO<sub>3</sub> Isomers**

molecule	A <sub>1</sub> (O <sub>c</sub> -O <sub>c</sub> )	A <sub>1</sub> (Ni-O <sub>c</sub> ) E' (Ni-O)	A <sub>1</sub> (Ni-O <sub>b</sub> ) A' <sub>1</sub> (Ni-O)	B <sub>1</sub> (Ni-O <sub>b</sub> ) E' bend	B <sub>1</sub> bend A <sub>2</sub> '' bend	B <sub>2</sub> bend
ONi(O <sub>2</sub> ) <sup>a</sup> C <sub>2v</sub> triplet <sup>b</sup>	1247 (115) 1176 (102) <sup>c</sup>	822 (6) 788 (5) <sup>c</sup>	569 (0) 540 (0)	520 (0) 495 (0)	39 (6) 38 (0)	116 (10) 112 (9)
ONiOO <sup>d</sup> bent singlet	1429 (210) 1349 (185) <sup>c</sup>	906 (67) 869 (64)	575 (6) 546 (5)	396 (0) 379 (0)	370 (0) 353 (0)	122 (9) 116 (0)
NiO <sub>3</sub> <sup>e</sup> D <sub>3h</sub> triplet		856 (19) 821 (18) <sup>c</sup>	777 (0) 731 (0)	274 (0) 263 (0)	150 (13) 149 (12)	

<sup>a</sup> Optimized structure for ONi(O<sub>2</sub>): R(Ni-O<sub>i</sub>) = 1.653 Å, R(Ni-O<sub>c</sub>) = 1.829 Å, ∠O<sub>i</sub>NiO<sub>i</sub> = 159°, ∠O<sub>c</sub>NiO<sub>c</sub> = 43°; O<sub>i</sub> and O<sub>c</sub> are terminal and "cyclic" oxygens. <sup>b</sup> The singlet and quintet states are higher by 11 and 16 kcal/mol, respectively. <sup>c</sup> The second frequency and intensity are given for <sup>18</sup>O-enriched isotopic molecule. <sup>d</sup> For ONiOO, R(Ni-O<sub>i</sub>) = 1.626 Å, R(Ni-O<sub>c</sub>) = 1.657 Å, R(O-O) = 1.269 Å, ∠O<sub>i</sub>-Ni-O = 159°, ∠Ni-O-O = 152°. <sup>e</sup> For NiO<sub>3</sub>, R(Ni-O) = 1.629 Å; NiO<sub>3</sub> is 21 kcal/mol higher than triplet ONi(O<sub>2</sub>).

**TABLE 4: DFT Calculated Frequencies (cm<sup>-1</sup>) and Intensities (km/mol) for NiO<sub>4</sub> Isomers**

(O <sub>2</sub> )Ni(O <sub>2</sub> ) <sup>a</sup> C <sub>2h</sub> triplet (almost D <sub>2h</sub> ) 0 kcal/mol	(O <sub>2</sub> )Ni(O <sub>2</sub> ) <sup>b</sup> C <sub>2h</sub> singlet (almost D <sub>2h</sub> ) +6 kcal/mol	(O <sub>2</sub> )NiOO <sup>c</sup> C <sub>1</sub> triplet +21 kcal/mol	(O <sub>2</sub> )NiO <sub>2</sub> <sup>d</sup> C <sub>1</sub> triplet (almost C <sub>2v</sub> ) +68 kcal/mol
1210 (1) O-O A <sub>g</sub>	1208 (3) O-O A <sub>g</sub>	1339 (182) O <sub>t</sub> -O <sub>t</sub> A'	1142 (175) O <sub>c</sub> -O <sub>c</sub> A <sub>1</sub>
1140 (1) <sup>e</sup>	1139 (2) <sup>e</sup>	1267 (168) <sup>e</sup>	1078 (156) <sup>e</sup>
1179 (273) O-O B <sub>u</sub> (FR)	1159 (387) O-O B <sub>u</sub>	1157 (256) O <sub>c</sub> -O <sub>c</sub> A'	830 (44) Ni-O <sub>t</sub> B <sub>2</sub>
1112 (242)	1094 (355)	1092 (236)	795 (40)
598 (4) Ni-O A <sub>g</sub> (FR)	726 (0) Ni-O B <sub>u</sub>	621 (4) Ni-O <sub>t</sub> A'	789 (26) Ni-O <sub>t</sub> A <sub>1</sub>
582 (5)	697 (0)	603 (3)	755 (24)
557 (3) Ni-O B <sub>u</sub>	673 (0) Ni-O B <sub>u</sub>	521 (0) Ni-O <sub>c</sub> A'	596 (5) Ni-O <sub>c</sub> B <sub>1</sub>
531 (12)	651 (0)	496 (0)	566 (4)
556 (10) Ni-O B <sub>u</sub> (FR)	504 (0) Ni-O A <sub>g</sub>	475 (1) Ni-O <sub>c</sub> A''	432 (11) Ni-O <sub>b</sub> A <sub>1</sub>
525 (0)	476 (0)	449 (0)	412 (10)
494 (0) Ni-O A <sub>g</sub>	476 (0) Ni-O A <sub>g</sub>	353 (0) bend A'	269 (2) bend A <sub>1</sub>
466 (0)	448 (0)	335 (0)	256 (1)
263 (2) twist bend	365 (0) twist bend A <sub>u</sub>	212 (5) bend A'	212 (5) bend A <sub>2</sub>
249 (0) A <sub>u</sub>	344 (0)	204 (4)	203 (3)
218 (1) in plane	234 (1) in plane	106 (3) bend A''	168 (12) bend B <sub>1</sub>
209 (0) bend A <sub>u</sub>	225 (0) bend A <sub>u</sub>	102 (2)	160 (10)
131 (7) out of plane	153 (7) out of plane	86 (3) bend A''	77 (4) bend B <sub>2</sub>
127 (5) bend B <sub>u</sub>	149 (5) bend B <sub>u</sub>	84 (3)	73 (3)

<sup>a</sup> Optimized geometry for triplet: R(Ni-O<sub>1</sub>) = R(Ni-O<sub>3</sub>) = 1.835 Å, R(Ni-O<sub>2</sub>) = R(Ni-O<sub>4</sub>) = 1.808 Å, ∠O<sub>1</sub>NiO<sub>2</sub> = ∠O<sub>3</sub>NiO<sub>4</sub> = 43.5°, R(O<sub>1</sub>-O<sub>2</sub>) = R(O<sub>3</sub>-O<sub>4</sub>) = 1.351 Å, (FR) denotes the bands involved in Fermi resonance. <sup>b</sup> Optimized geometry for singlet: R(Ni-O<sub>1</sub>) = R(Ni-O<sub>3</sub>) = 1.823 Å, R(Ni-O<sub>2</sub>) = R(Ni-O<sub>4</sub>) = 1.793 Å, ∠O<sub>1</sub>NiO<sub>2</sub> = ∠O<sub>3</sub>NiO<sub>4</sub> = 44.0°, R(O<sub>1</sub>-O<sub>2</sub>) = R(O<sub>3</sub>-O<sub>4</sub>) = 1.355 Å. <sup>c</sup> R(Ni-O<sub>c</sub>) = 1.83 Å, R(Ni-O<sub>i</sub>) = 1.705 Å, R(O<sub>1</sub>-O<sub>2</sub>) = 1.291 Å, ∠O<sub>c</sub>NiO<sub>i</sub> = 158°, ∠O<sub>c</sub>NiO<sub>c</sub> = 43°, ∠NiO<sub>i</sub>O<sub>2</sub> = 144°, tetrahedral angle between O<sub>2</sub> and O<sub>c</sub>NiO<sub>i</sub> plane is 144° O<sub>c</sub> = "cyclic" oxygens, O<sub>1,2</sub> = oxygens of NiOO fragment. <sup>d</sup> Optimized geometry: R(Ni-O<sub>t1</sub>) = 1.659 Å, R(Ni-O<sub>t2</sub>) = 1.647 Å, R(Ni-O<sub>c1</sub>) = 1.901 Å, R(Ni-O<sub>c2</sub>) = 1.776 Å, ∠O<sub>t1</sub>NiO<sub>t2</sub> = 114°, ∠O<sub>c1</sub>NiO<sub>c2</sub> = 43°, tetrahedral angles between O<sub>t1</sub>, O<sub>t2</sub> and O<sub>c1</sub>NiO<sub>c2</sub> plane are 100 and 97°. O<sub>t1,t2</sub> = terminal oxygens, O<sub>c1,c2</sub> = "cyclic" oxygens. <sup>e</sup> The second frequency and intensity are given for <sup>18</sup>O-enriched isotopic molecule.

Reaction 1 is 30 ± 3 kcal/mol endothermic, based on D(NiO) = 88 ± 3 kcal/mol,<sup>6,22</sup> which requires excess energy from hollow cathode sputtering<sup>5</sup> or laser ablation sources (e.g., 10 eV)<sup>3</sup> of energetic Ni atoms.

It is interesting to note the absence of a NNNiO complex, particularly in N<sub>2</sub>O experiments, where the analogous NNFeO complex gave a strong absorption which increased on annealing.<sup>2</sup>

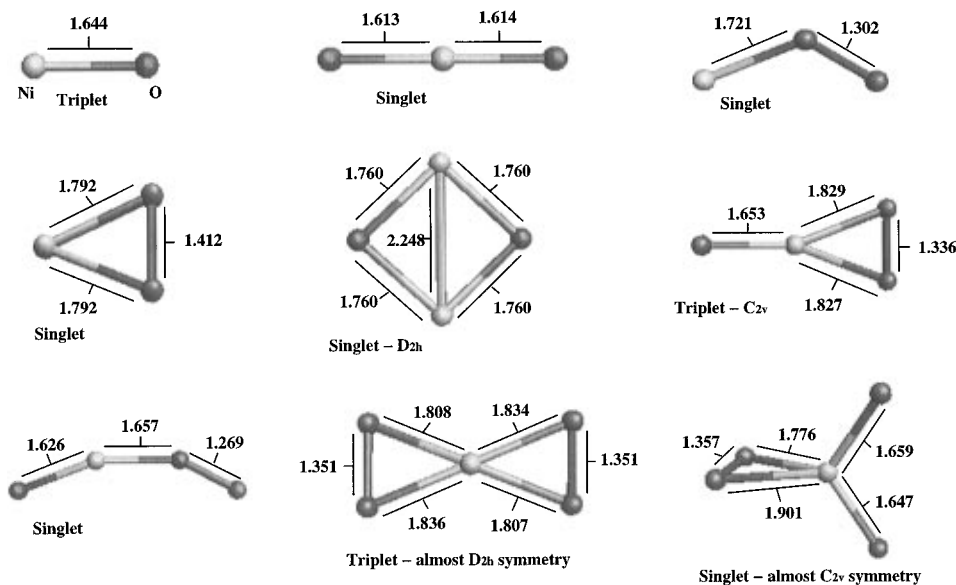
**NiO<sub>2</sub>. ONiO Molecule.** Two sharp bands 954.9 and 949.3 cm<sup>-1</sup> with intensity distribution 2.5:1.0 were observed in argon matrices after deposition; a weaker associated 944.1 cm<sup>-1</sup> band in higher yield experiments is appropriate for the <sup>62</sup>Ni (3.7%)

in natural abundance. The resolved nickel isotopic splittings show that this vibration involves a single Ni atom. The 954.9 cm<sup>-1</sup> band produced a triplet isotopic structure with scrambled oxygen, which characterizes the vibration of two equivalent oxygen atoms. The 16/18 ratio 1.0373 is very close to the calculated harmonic value (1.0379) for  $\nu_3$  of a linear ONiO molecule, and the 58/60 ratio (1.005 90) is also close to the calculated harmonic ratio (1.005 98). The 954.9 cm<sup>-1</sup> band is assigned to  $\nu_3$  of the linear insertion product O<sup>58</sup>NiO molecule. Note that present assignment is in an excellent agreement with DFT calculations, which gave 1027 cm<sup>-1</sup> for the  $\nu_3$  vibration of linear nickel dioxide. Note also that asymmetry in the oxygen

**TABLE 5: DFT Calculated Frequencies ( $\text{cm}^{-1}$ ) and Intensities ( $\text{km/mol}$ ) for Rhombic  $\text{Ni}_2\text{O}_2$  States**

state	$A_g$ Ni–O	$B_{2u}$ Ni–O	$B_{3u}$ Ni–O	$B_{1g}$ Ni–O	$B_{1u}$ bend	$A_g$ Ni–Ni
singlet <sup>a</sup>	784 (0)	709 (45)	556 (42)	547 (0)	387 (22)	378 (0)
0.2 kcal/mol	742 (0) <sup>b</sup>	678 (41)	532 (38)	525 (0)	370 (20)	377 (0)
triplet <sup>c</sup>	795 (0)	633 (339)	526 (34)	524 (2)	275 (7)	424 (1)
0 kcal/mol	752 (0) <sup>b</sup>	605 (307)	503 (14)	502 (2)	263 (6)	422 (0)

<sup>a</sup>  $R(\text{Ni}-\text{O}) = 1.760 \text{ \AA}$ ,  $\angle\text{ONiO} = 101^\circ$ . <sup>b</sup> The second frequency and intensity are given for  $^{18}\text{O}$ -enriched isotopic molecule. <sup>c</sup>  $R(\text{Ni}-\text{O}) = 1.763 \text{ \AA}$ ,  $\angle\text{ONiO} = 104^\circ$ .

**Figure 5.** Optimized structures for nickel oxide product molecules. Bond distances are in angstroms.

isotopic triplet ( $15.4\text{--}19.0 \text{ cm}^{-1}$ ) points to a nearby lower  $\nu_1$  mode, which is predicted at  $805 \text{ cm}^{-1}$  by DFT calculations. The present assignment of a  $954.9/949.3 \text{ cm}^{-1}$  nickel isotopic doublet to linear ONiO differs with a tentative assignment reported by the Moscow group.<sup>23</sup> If the scale factor (0.93) that converts the calculated  $\nu_3$  to the observed value is applied to  $\nu_1$ , a  $748 \text{ cm}^{-1}$  value is predicted. These frequencies for ONiO ( $955, 748 \text{ cm}^{-1}$ ) compare favorably with the stretching fundamentals for linear OCuO ( $823, 658 \text{ cm}^{-1}$ ) and bent OFeO ( $946, 797 \text{ cm}^{-1}$ ).<sup>1,2,24</sup>

In nitrogen experiments the similar doublet at  $959.5/953.9 \text{ cm}^{-1}$  also produced triplets in an experiment with the statistical oxygen isotopic mixture. The 16/18 and 58/60 isotopic ratios (1.0375 and 1.00587) are again very close to the harmonic values for linear ONiO. This doublet is due to the linear nickel dioxide molecule completely surrounded by nitrogen molecules.

$\text{Ni}(\text{O}_2)$ . The  $967.1 \text{ cm}^{-1}$  band appeared in the spectra after deposition in experiments with high oxygen concentration or it was observed after annealing in experiments with low oxygen concentration. Triplet oxygen isotopic structure with the 16/18 ratio 1.0575 shows that the leading candidate should be  $\text{Ni}(\text{O}_2)$ , which agrees with the previous assignment of a  $966.2 \text{ cm}^{-1}$  band to this molecule.<sup>11</sup> Two weak nickel isotopic doublets  $538.3/535.3$  and  $511.7/510.9 \text{ cm}^{-1}$  in the low-frequency region behaved similarly after deposition and annealing and also produced triplets with scrambled oxygen and the 16/18 ratios 1.0374 and 1.0535, respectively. For the  $\text{Ni}(\text{O}_2)$  molecule with a  $40^\circ$  valence ONiO angle, the estimated 16/18 ratios for the  $\nu_2$  and  $\nu_3$  vibrations are 1.0397 and 1.0568, respectively, which are very close to the experimental ratios. Moreover, the estimated 58/60 ratios are 1.00551 and 1.00101, which are comparable to the experimental values 1.0056 and 1.00157. (All estimates were made neglecting off-diagonal  $\mathbf{G}$  matrix elements.) Thus, these bands are assigned to  $\nu_2$  and  $\nu_3$  vibrations of the  $\text{Ni}(\text{O}_2)$  molecule. Note that the previous work

assigned 505 and  $535 \text{ cm}^{-1}$  bands to the  $\text{Ni}(\text{O}_2)$  and  $\text{Ni}(\text{O}_2)_2$  molecules;<sup>11</sup> our experiments did not reveal the first band, and we reassign the second one. The DFT calculations (Table 2) predicted a weaker  $\nu_2$  mode at  $599.2 \text{ cm}^{-1}$  and a stronger  $\nu_3$  mode at  $477.8 \text{ cm}^{-1}$  with calculated 16/18 ratios 1.0396 and 1.0542, respectively, for the singlet  $\text{Ni}(\text{O}_2)$  state. Similarly, the  $\nu_1$  mode is predicted at  $1029 \text{ cm}^{-1}$ . These 16/18 ratios are in excellent agreement with the observed values, and the DFT calculations confirm the assignment of all three modes of cyclic  $\text{Ni}(\text{O}_2)$ . This is the only transition metal peroxo species for which all three normal modes are known.

The low  $967 \text{ cm}^{-1}$  O–O mode frequency suggests that the  $\text{Ni}(\text{O}_2)$  molecule is more of a peroxide rather than superoxide but still not as low as  $\text{Ca}(\text{O}_2)$  at  $742 \text{ cm}^{-1}$ .<sup>25</sup> Note that the 16/18 ratio for this mode, 1.0575, is less than expected for an O–O stretching mode, which also was found for cyclic  $\text{Fe}(\text{O}_2)$  at  $956 \text{ cm}^{-1}$ . In the case of  $\text{Fe}(\text{O}_2)$  this decrease was explained by strong coupling of symmetric O–O and  $\text{Fe}-\text{O}_2$  stretching vibrations.<sup>1,2</sup> This coupling is apparently less for  $\text{Ni}(\text{O}_2)$ .

DFT calculations for triplet cyclic  $\text{Ni}(\text{O}_2)$  gave  $1038 \text{ cm}^{-1}$  for the O–O vibration, which is in also accord with the experimental assignment. However, the calculated  $\nu_2$  and  $\nu_3$  modes disagree with experiment, which shows that the singlet  $\text{Ni}(\text{O}_2)$  is in fact observed here, even though the DFT calculations predict the triplet state to be 3 kcal/mol lower. For both ONiO and  $\text{Ni}(\text{O}_2)$  the same factor 0.93 can be applied to scale the DFT calculated  $\nu_3$  and  $\nu_1$  modes to experimental values, respectively.

In solid nitrogen the  $970.1 \text{ cm}^{-1}$  band gave triplet isotopic structure with the 16/18 ratio 1.0556, which differs slightly from the argon value. Recall that the 977 and  $972 \text{ cm}^{-1}$  bands were observed previously<sup>13</sup> and in this work with the  $\text{Ni} + \text{O}_2/\text{N}_2/\text{Ar}$  system and assigned to the  $\text{N}_2\text{Ni}(\text{O}_2)$  and  $(\text{N}_2)_2\text{Ni}(\text{O}_2)$  molecules; experimental isotopic ratios for these bands were 1.0562 and 1.0565. In other words, increasing the number of complexed

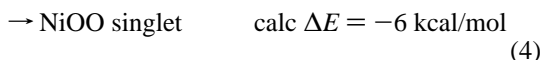
dinitrogen groups leads to decreasing the O–O frequency. In solid N<sub>2</sub> the Ni(O<sub>2</sub>) molecule is completely surrounded by nitrogen, and the 970.1 cm<sup>-1</sup> band should be attributed to (N<sub>2</sub>)<sub>n</sub>-Ni(O<sub>2</sub>). Note that both ONiO and Ni(O<sub>2</sub>) show small blue shifts from solid argon to solid nitrogen. This is in contrast to OFeO and Fe(O<sub>2</sub>) which show larger red shifts.<sup>14</sup>

*NiOO*. The band 1221.3 cm<sup>-1</sup> was observed in argon matrices after annealing and produced three bands with the statistical mixture with the central component partially resolved into two bands at 1188.0 and 1187.7 cm<sup>-1</sup>. The 16/18 ratio 1.0582 indicates an O–O vibration, and following the iron–oxygen system, this band is assigned to the NiOO molecule. For the analogous FeOO molecule isotopic splitting for intermediate bands was only 2.6 cm<sup>-1</sup>, and this splitting should decrease with increasing mass of the metal atom. The DFT calculated frequency 1226 cm<sup>-1</sup> is very close to the experimental value, which may be fortuitous in comparison with calculated frequencies for the ONiO and Ni(O<sub>2</sub>) molecules. The Ni–O stretching mode predicted at 622 cm<sup>-1</sup> is too weak to be observed.

Thus, three NiO<sub>2</sub> isomers, linear ONiO, cyclic Ni(O<sub>2</sub>), and asymmetric NiOO, coexist in argon matrices, the same as found for iron.<sup>1,2</sup> It is interesting that in experiments with mechanical isotopic mixtures all isomers produced doublet isotopic structures. This means that the main mechanism of formation is reaction between Ni atoms and oxygen molecules and not reaction of nickel monoxide and atomic oxygen (or ozone). The linear isomer is formed during deposition in the gas phase near the matrix surface by direct insertion:



This reaction requires activation energy, and only high kinetic energy metal atoms can insert into the oxygen molecule, which explains why ONiO was not observed in thermal experiments.<sup>11</sup> However, these bands increase slightly on annealing to 20–30 K and then decrease thereafter (Figure 1). This means a minor contribution to the yield of ONiO can arise from the O + NiO reaction on annealing. The formation of cyclic and asymmetric isomers does not require activation energy, and reactions 3 and 4 occur spontaneously on annealing:



The energy changes are from the present DFT calculations, which might be in error by as much as 10 kcal/mol.

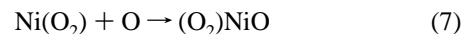
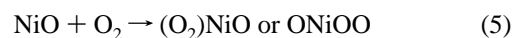
**ONiO<sup>-</sup>**. The weak 2.5:1.0 doublets 886.8/881.6 and 894./889.2 cm<sup>-1</sup> were detected in solid argon and nitrogen, respectively, after deposition with high laser power. These bands were not affected by broad-band photolysis, but they decreased on annealing. The 16/18 and 58/60 ratios 1.0374/1.0379, 1.0373/1.0378, 1.005 90, and 1.005 85 together with 1:2:1 oxygen isotopic structure indicate another linear molecule with one nickel and two equivalent oxygen atoms. The 60 cm<sup>-1</sup> frequency shift from the ONiO molecule and annealing behavior do not associate these bands with any complex of ONiO and O<sub>2</sub>. The anion ONiO<sup>-</sup> is suggested for these bands. Similar isotopic ratios to the neutral ONiO indicate that the molecule does not bend attaching an electron, as expected since the isoelectronic OCuO molecule is linear.<sup>24</sup> Analogous frequency relationships were found for Ti, Zr, and Hf dioxides and their anions.<sup>26</sup>

**NiO<sub>3</sub>**. (*O*<sub>2</sub>)NiO. A weak 1095.5 cm<sup>-1</sup> band observed in argon increased markedly on annealing. This band was stronger in experiments with a higher yield of NiO. In statistical <sup>16,18</sup>O<sub>2</sub> experiments, a sharp 1095.5, 1065.6, 1034.6 cm<sup>-1</sup> triplet was observed, which produced the 16/18 ratio 1.0584. DFT calculations predict one strong O–O stretching vibration at 1247 cm<sup>-1</sup> and a very weak Ni–O stretching mode at 822 cm<sup>-1</sup>, which is not observed. This is reasonable agreement to support identification of triplet state (*O*<sub>2</sub>)NiO; a scale factor of 0.88 is required whereas a 0.94 scale factor is determined for this mode of singlet Ni(O<sub>2</sub>).

*ONiOO*. A sharp new 1393.7 cm<sup>-1</sup> band appeared on annealing, disappeared on photolysis, and reappeared on further annealing. This band gave two oxygen-18 counterparts, 1322.7 and 1301.8 cm<sup>-1</sup>, each with clear nickel isotopic splittings. The mechanical mixture revealed the <sup>16</sup>O<sub>2</sub> plus the <sup>18</sup>O<sub>2</sub> spectra and two additional 1391.1 and 1309.3 cm<sup>-1</sup> bands (Figure 2). Four statistical <sup>16,18</sup>O<sub>2</sub> experiments produced the four additional bands at 1368.5, 1361.2, 1348.6, and 1339.4 cm<sup>-1</sup>. Fermi resonance, which also complicates the spectrum of (*O*<sub>2</sub>)Ni(O<sub>2</sub>), gives a strong extra band for the oxygen-18 species and weak extra bands for the oxygen-16 species and one mixed isotopic molecule. The remaining “octet” absorption profile clearly indicates a vibration of two inequivalent oxygen atoms coupled to a third inequivalent oxygen atom. This pattern identifies the ONiOO isomer. DFT calculations predict a very strong O–O stretching mode at 1429 cm<sup>-1</sup>, in excellent agreement.

The above Fermi resonance involves the O–O stretching fundamental and the combination of terminal O–NiOO and internal ONi–OO stretching modes as is demonstrated by nickel isotopic splittings and DFT calculations. A pure Ni–<sup>18</sup>O stretching mode at 1312 cm<sup>-1</sup> would exhibit a <sup>58</sup>Ni–<sup>60</sup>Ni splitting of 5.2 cm<sup>-1</sup>; the nickel isotopic shifts in the 1322.7 cm<sup>-1</sup> and 1301.8 cm<sup>-1</sup> components of the Fermi doublet are 2.8 and 2.5 cm<sup>-1</sup>, which show that the two components are about half Ni–O stretching overtone and O–O stretching fundamental. On the other hand a pure Ni–<sup>16</sup>O stretching mode at 1380 cm<sup>-1</sup> would show a nickel isotopic splitting of 4.8 cm<sup>-1</sup>; the observed splittings were 1.0 and 3.9 cm<sup>-1</sup> for the stronger 1393.7 cm<sup>-1</sup> and weaker 1367.1 cm<sup>-1</sup> bands. This demonstrates a weaker Fermi resonance interaction in the oxygen-16 species and predicts unshifted bands near 1389 and 1373 cm<sup>-1</sup> for the O–O stretching fundamental and the Ni–O combination band. The Ni–O fundamentals calculated at 906 and 575 cm<sup>-1</sup> (Table 3) were too weak to observe. The 1389/1312 = 1.0587 and 1373/1312 = 1.0465 ratios are appropriate 16/18 ratios for these modes and in good agreement with the 1.0593 and 1.0461 ratios of the calculated isotopic frequencies.

Note that the O–O stretching mode in ONiOO (1393.7 cm<sup>-1</sup>) is not reduced as far as that in NiOO (1221.3 cm<sup>-1</sup>) as is the case for ONi(O<sub>2</sub>) (1095.5 cm<sup>-1</sup>) compared to Ni(O<sub>2</sub>) (967.1 cm<sup>-1</sup>). Clearly, Ni is a better reducing agent than NiO as the first available electrons on Ni (4s<sup>2</sup>) are involved in bonding to the oxide oxygen. Three reactions can lead to (*O*<sub>2</sub>)NiO or ONiOO formation:



Based on relative of intensities of NiO bands, the first reaction appears to be more important. In this regard, weak bands that grew on annealing at 795, 786 cm<sup>-1</sup> have the proper 16/18 ratio

(1059) for  $\text{Ni}^+\text{O}_3^-$  ozonide species. We note that  $\text{Cu}^+\text{O}_3^-$  ozonide was a much more dominant species in the copper system.<sup>24c</sup>

**NiO<sub>4</sub>.** ( $\text{O}_2$ )Ni( $\text{O}_2$ ). The 1063.9  $\text{cm}^{-1}$  band was observed in argon matrices after annealing. Oxygen-18 isotopic substitution revealed that the  $^{18}\text{O}$  counterpart of this band is at 1009.9  $\text{cm}^{-1}$  (Figure 3); however, note the nickel isotopic splittings on these bands at 1062.6 and 1007.7  $\text{cm}^{-1}$ . The  $^{16}\text{O}_2 + ^{18}\text{O}_2$  experiment revealed the same bands plus *two* new bands at 1078.1 and 1002.6  $\text{cm}^{-1}$ , which are *above and below* the  $^{16}\text{O}_2$  and  $^{18}\text{O}_2$  counterparts, respectively. Moreover, eight isotopic components were found in experiments with the statistical mixture, and nickel isotopic splittings were observed for six of these. These results disagree, in part, with those reported earlier where 1062.0 and 1001.4  $\text{cm}^{-1}$  bands were assigned to the  $^{16}\text{O}$  and  $^{18}\text{O}$  counterparts of a "spiro"  $D_{2d}$  ( $\text{O}_2$ )Ni( $\text{O}_2$ ) molecule, respectively, and a sextet mixed isotopic structure was claimed.<sup>11</sup> The difference between  $^{16}\text{O}$  counterparts is only 1.9  $\text{cm}^{-1}$  and may be explained by instrument calibration, but we assign a different band to the  $^{18}\text{O}$  counterpart and observe more mixed isotopic absorptions; the mixed isotopic bands at 1082.2 and 1078.1  $\text{cm}^{-1}$  were not reported.<sup>11</sup> The mixed isotopic band at 1002.6  $\text{cm}^{-1}$  is close to the 1001.4  $\text{cm}^{-1}$  band assigned to ( $^{18}\text{O}_2$ )Ni( $^{18}\text{O}_2$ ) in the previous work. Note that the present and previous ( $^{16}\text{O}_2$ )-Ni( $^{16}\text{O}^{18}\text{O}$ ) and ( $^{16}\text{O}^{18}\text{O}$ )Ni( $^{16}\text{O}^{18}\text{O}$ ) counterparts coincide within 1.5  $\text{cm}^{-1}$  (1045.2 and 1046.2  $\text{cm}^{-1}$ , 1035.2 and 1036.6  $\text{cm}^{-1}$ , respectively), but the ( $^{16}\text{O}_2$ )Ni( $^{18}\text{O}_2$ ) and ( $^{18}\text{O}_2$ )Ni( $^{16}\text{O}^{18}\text{O}$ ) assignments disagree: instead of the 1018.2 and 1016.2  $\text{cm}^{-1}$  bands, assigned earlier, the 1002.6 and 1019.1  $\text{cm}^{-1}$  bands are here assigned to these isotopic molecules. Finally, the weak band at 535  $\text{cm}^{-1}$ , assigned earlier to ( $\text{O}_2$ )Ni( $\text{O}_2$ ), has been reassigned here to Ni( $\text{O}_2$ ).

As mentioned above, several NiO<sub>4</sub> structures were calculated, and it was found that a planar  $C_{2h}$  molecule (almost  $D_{2h}$ ) is the most stable isomer instead of the  $D_{2d}$  isomer. From Table 4 it is easy to see that  $\nu\text{B}_u(\text{O}-\text{O})$  and  $\nu\text{B}_u(\text{Ni}-\text{O}) + \nu\text{A}_g(\text{Ni}-\text{O})$  vibrations are close, which can lead to Fermi resonance. Note that the difference between these levels is smaller for the  $^{18}\text{O}$ -enriched molecule. Although mixed components were not calculated, it is suggested that this difference is even smaller for some of them. Based on this interpretation, the extra isotopic structure is explained. The 1082.2/1019.1 and 1078.1/1002.6  $\text{cm}^{-1}$  bands are Fermi doublets for the ( $^{16}\text{O}_2$ )Ni( $^{16}\text{O}^{18}\text{O}$ ) and ( $^{16}\text{O}_2$ )Ni( $^{18}\text{O}_2$ ) molecules.

The calculated 1179  $\text{cm}^{-1}$   $\text{B}_u$  band is out-of-phase O–O stretching whereas the 598  $\text{cm}^{-1}$   $\text{A}_g$  band is an antisymmetric combination of symmetric Ni–O<sub>2</sub> stretching and the 556  $\text{cm}^{-1}$   $\text{B}_u$  band is an antisymmetric combination of antisymmetric Ni–O<sub>2</sub> stretching modes as the 16/18 ratios indicate. The weak doublet 1001.4, 998.2  $\text{cm}^{-1}$  that tracks with the strong 1063.9, 1062.6  $\text{cm}^{-1}$  doublet are Fermi resonance pairs. Note the sum of nickel isotopic shifts is 4.5  $\text{cm}^{-1}$ , close to that expected for Ni–O stretching in this region. The 16/18 ratios for the Ni–O combination band and the O–O stretch should be 1.0434 and 1.0602, respectively, in the absence of Fermi resonance. The observed 16/18 ratios, 1.0471 and 1.0535, show the effect of mode mixing through Fermi resonance.

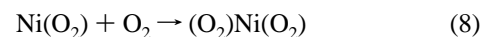
The ( $\text{O}_2$ )Ni( $\text{O}_2$ ) molecule provides an interesting case for the examination of Fermi resonance through isotopic substitution. The strong 1063.9  $\text{cm}^{-1}$  absorption shows a 1.3  $\text{cm}^{-1}$  Ni isotopic shift, but the weak 1001.4  $\text{cm}^{-1}$  band shows a 3.2  $\text{cm}^{-1}$  Ni isotopic shift. If the 1063.9  $\text{cm}^{-1}$  band were a pure O–O stretch, no Ni isotopic shift would be observed, and the ( $^{18}\text{O}_2$ )-Ni( $^{18}\text{O}_2$ ) counterpart would be at 1003.5  $\text{cm}^{-1}$ , which falls close to the combination band. The oxygen-18 counterpart is blue-shifted to 1009.9  $\text{cm}^{-1}$ , and the combination band is red-shifted

more than mass alone could have done. The 1009.9  $\text{cm}^{-1}$  band shows a 2.2  $\text{cm}^{-1}$  Ni isotopic shift and the 955.8  $\text{cm}^{-1}$  band only a 2.6  $\text{cm}^{-1}$  shift, indicating more mode mixing and intensity sharing with the oxygen-18 species. The ( $^{16}\text{O}_2$ )Ni( $^{16}\text{O}^{18}$ ) and ( $^{16}\text{O}_2$ )Ni( $^{18}\text{O}_2$ ) isotopic molecules sustain a particularly strong interaction as these Fermi doublet component intensities are comparable. The mixing of metal participation in the O–O stretching mode can be followed here by the  $^{58}\text{Ni}$ – $^{60}\text{Ni}$  isotopic shift.

Another possible consideration is that a different ( $\text{O}_2$ )Ni( $\text{O}_2$ ) isomer was formed in our experiments. But, no stoichiometry or structure can be proposed to explain the appearance of 1082.2, 1078.1, and 1002.6  $\text{cm}^{-1}$  bands, which are above and below the  $^{16}\text{O}$  and  $^{18}\text{O}$  counterparts, respectively. Hence, Fermi resonance complicates the isotopic spectrum of ( $\text{O}_2$ )Ni( $\text{O}_2$ ) which was not appreciated in the earlier work.<sup>11</sup>

( $\text{O}_2$ )NiO<sub>2</sub>. The 1135.8 and 851.0/848.0  $\text{cm}^{-1}$  bands were observed in argon after annealing or after deposition with high laser power and oxygen concentration. These bands were stronger after deposition when the ONiO band was strong. Isotopic substitution revealed a broad triplet with the 16/18 ratio 1.0589 for the upper band, which is assigned to the O–O vibration of the ( $\text{O}_2$ )NiO<sub>2</sub> molecule. DFT calculations predict a  $C_1$  (almost  $C_{2v}$ ) structure for this molecule, with a strong O–O stretching mode and a weaker Ni–O stretching mode. The Ni isotopic doublet at 851.0/848.0  $\text{cm}^{-1}$  is appropriate for this molecule.<sup>27</sup> Another possible assignment is to the ( $\text{O}_2$ )NiOO molecule, but calculations predict two strong O–O stretches in the high frequency region (Table 4), and this assignment seems less probable.

The correlation of the 1063.9 and 1135.8  $\text{cm}^{-1}$  bands with bands of Ni( $\text{O}_2$ ) and ONiO, respectively, and the pronounced growth on annealing suggests that the two NiO<sub>4</sub> isomers are formed by the following secondary reactions:



**Ni<sub>2</sub>O.** Two doublets 844.6/842.6  $\text{cm}^{-1}$  (Ar) and 849.5/847.5  $\text{cm}^{-1}$  (N<sub>2</sub>) with intensity distribution 3:1 appeared in the spectra after deposition with high laser power and decreased after annealing. The doublet in nitrogen was a little bit stronger than in argon; with oxygen isotopic substitution, doublets with ratios 1.0497 and 1.0495 were observed. Concentration dependence, oxygen isotopic structure, and annealing behavior suggest that this molecule contains more than one nickel atom but only one oxygen atom. The Ni<sub>2</sub>O molecule is suggested, but the 3/1 Ni isotopic doublet shows that only one Ni atom is involved in the vibration. Hence, the structure NiNiO is suggested. The dimer Ni<sub>2</sub> has been observed in solid argon and a 2.78 eV dissociation energy calculated.<sup>28,29</sup> Accordingly, the 844.6/842.6  $\text{cm}^{-1}$  doublet is tentatively assigned to NiNiO.

**Ni<sub>2</sub>O<sub>2</sub>.** ( $\text{NiO}$ )<sub>2</sub>. The broad weak band 654.2  $\text{cm}^{-1}$  was observed after deposition and decreased on annealing. After isotopic substitution it gave a 1:1:1 asymmetric set of bands at 654.2, 632.8, 625.5  $\text{cm}^{-1}$  plus a new 676.2  $\text{cm}^{-1}$  band. The 16/18 ratio 1.0459 is very close to the diatomic value, so the  $\text{B}_{2u}$  mode in a rhombic dimer must be considered. For such a molecule the antisymmetric stretching vibrations are infrared active, but isotopic substitution leads to lowering of symmetry and the symmetric stretching mode of Ni<sup>16</sup>ONi<sup>18</sup>O may be observed with intensity depending upon mode mixing (which appeared as asymmetry in the isotopic structure). Moreover, the presence of coupling will shift intensity distribution from 1:2:1 triplet to a 1:1:1:1 quartet, which was observed here.



A weak 7:5:1 triplet at 650.2/649.0/648.0  $\text{cm}^{-1}$  revealed a similar asymmetric triplet with statistical isotopic oxygen, which is appropriate for the vibration of two equivalent Ni atoms and two equivalent O atoms in a better isolated matrix site. This band decreased on annealing with the 654.2  $\text{cm}^{-1}$  band, while a weak 614.4/613.3/612.4  $\text{cm}^{-1}$  triplet appeared with the same isotopic ratios.

The broad low-frequency bands at 485.1 and 481.6  $\text{cm}^{-1}$  appeared in the spectra after deposition and decreased after annealing; the latter band showed a hint of unresolved nickel isotopic splitting like the 650.2, 649.0, 648.0  $\text{cm}^{-1}$  bands. Oxygen isotopic substitution revealed a 1:2:1 triplet with the 16/18 ratio 1.0468, which is very close to the diatomic value. Appearance of oxygen isotopic triplets for the 485.1 and 481.6  $\text{cm}^{-1}$  bands indicates that this product also contains two equivalent oxygen atoms. The 654.2 and 485.1  $\text{cm}^{-1}$  band systems decrease together on annealing and must be considered for the same molecule.

DFT calculations predict the singlet molecule to have comparable intensities for  $B_{2u}$  and  $B_{3u}$  vibrations, while for the triplet molecule only the  $B_{2u}$  vibration is strong enough to be observed. If this level of theory is adequate for singlet  $(\text{NiO})_2$ , the calculated  $B_{2u}$  and  $B_{3u}$  modes must be scaled by 0.92 and 0.87 to fit the observed bands, and the singlet  $(\text{NiO})_2$  state is probably observed here. We note a similar relationship between the bands for CaO and  $(\text{CaO})_2$  on one hand<sup>25</sup> and NiO and  $(\text{NiO})_2$  on the other.

The calculated Ni–Ni distance across the singlet ring is 2.248 Å, which is comparable to the 2.20 Å bond length for ground state  $\text{Ni}_2$ .<sup>30</sup> Clearly, part of the stability of  $(\text{NiO})_2$  derives from Ni–Ni bonding. In fact, the calculated low-frequency  $A_g$  mode (378  $\text{cm}^{-1}$  with 1  $\text{cm}^{-1}$  oxygen-18 shift) corresponds to the Ni–Ni stretching mode and is in agreement with the  $\text{Ni}_2$  fundamental (379  $\text{cm}^{-1}$ ) from the matrix fluorescence spectrum.<sup>28</sup> Finally, the dimerization energy of NiO is calculated by DFT to be exothermic by 82 kcal/mol.

**Bent NiONiO.** The triplet 973.9/972.4/970.8  $\text{cm}^{-1}$  was observed to grow strongly on annealing. Using  $^{18}\text{O}_2$ , the slightly broader intermediate band was resolved into two bands (Table 1), indicating the vibration of two inequivalent Ni atoms. With  $^{16}\text{O}_2 + ^{18}\text{O}_2$  only pure isotopic spectra were observed, but with the statistical mixture additional slightly displaced mixed oxygen isotopic bands were observed, denoting two inequivalent O atoms. A similar triplet blue-shifted by 1  $\text{cm}^{-1}$  was produced with  $\text{N}_2\text{O}$ . This band is in the terminal Ni–O vibration region and is appropriate for bent NiONiO. A similar CuOCuO molecule was observed 147  $\text{cm}^{-1}$  above linear OCuO in the spectrum of the Cu +  $\text{O}_2$  system.<sup>24c</sup>

It is interesting to consider possible pathways of  $\text{Ni}_2\text{O}_2$  isomer formation. Neither NiONiO nor  $(\text{NiO})_2$  revealed intermediate components with the mechanical isotopic mixture. This shows that the main mechanism is not dimerization of NiO but reaction of a second Ni atom with either  $\text{Ni}(\text{O}_2)$  or ONiO. The same conclusion was reached for the analogous  $(\text{FeO})_2$  and  $(\text{CoO})_2$  molecular species.<sup>2,31</sup>

**$\text{Ni}_2\text{O}_3$ .** ( $\text{Ni}_2\text{O}_2$ )O. The weak triplet that appeared at 614.4/613.3/612.4  $\text{cm}^{-1}$  involves two Ni atoms and exhibits an intermediate oxygen isotopic component. The 16/18 ratio is slightly higher than the diatomic value. Following the above identification of cyclic  $\text{Ni}_2\text{O}_2$ , these weak bands are tentatively assigned to  $(\text{Ni}_2\text{O}_2)\text{O}$ , a branched ring.

**ONiONiO.** The sharp 962.3/961.1/959.9  $\text{cm}^{-1}$  triplet appeared in the spectra after annealing. The 7:5:1 relative intensities denote the vibration of two equivalent Ni atoms. The triplet was not as well resolved with  $^{16}\text{O}_2 + ^{18}\text{O}_2$ , suggesting a

minor coupling. With statistical isotopic oxygen the band maxima were displaced inward to 961.1 and 920.7  $\text{cm}^{-1}$  suggesting a partially resolved sextet for two equivalent-inequivalent O atoms. The same triplet (blue-shifted 0.3  $\text{cm}^{-1}$ ) appeared on annealing in the  $\text{N}_2\text{O}$  experiment. The bent (or “W”-shaped) ONiONiO molecule is proposed to account for this sharp Ni isotopic triplet. A similar sharp 995.3/993.9/992.5  $\text{cm}^{-1}$  triplet has been assigned to nearly linear OCuOCuO.<sup>24c</sup>

**Other Absorptions.** The broad 1498.9  $\text{cm}^{-1}$  band that grows on annealing (16/18 ratio 1.0591) is due to the weakest O–O complex observed here. This weak complex has less effect on the O–O stretching mode than complexes with NiO and Ni, and it may arise from a higher oxide. The doublet at 951.5, 950.1  $\text{cm}^{-1}$  growing on annealing just below  $\text{Ni}_2\text{O}_3$  also involves two equivalent Ni atoms and is probably due to a perturbed  $\text{Ni}_2\text{O}_3$  species.

Oxygen chemisorbs dissociatively on the Ni(110) surface, even at low temperatures, and physisorbed  $\text{O}_2$  can be ruled out by the absence of molecular infrared absorptions.<sup>32</sup> How large does a  $\text{Ni}_x$  cluster have to be for dissociation to occur? One Ni atom is clearly not enough, as NiOO and  $\text{Ni}(\text{O}_2)$  are observed. In the case of  $\text{O}_2$  on Pt(111) a strong 860  $\text{cm}^{-1}$  band in the EEL spectrum suggests reduction to a O–O single-bond adsorbed species.<sup>33</sup> The broad 715  $\text{cm}^{-1}$  band that grows on annealing could be due to a nickel cluster–dioxygen species. The apparent  $^{18}\text{O}_2$  shift to 680  $\text{cm}^{-1}$  suggests some Ni–O character in the vibrational motion.

A weak 760.5/758.1  $\text{cm}^{-1}$  nickel isotopic doublet gave only the strongest band at 726.3  $\text{cm}^{-1}$  with  $^{18}\text{O}_2$ . This band is due to NNiO, as will be discussed more fully, along with NiN, in a later paper.

## Conclusions

The major differences between the reaction of laser-ablated and thermal Ni atoms with  $\text{O}_2$  are the formation of the nickel oxide species—NiO, ONiO, two  $\text{Ni}_2\text{O}_2$  isomers, and ONiONiO—with more energetic laser-ablated atoms, in addition to the cyclic  $\text{Ni}(\text{O}_2)$  and  $(\text{O}_2)\text{Ni}(\text{O}_2)$  addition products formed with thermal nickel atoms.<sup>11</sup> Dioxygen complexes are also formed with NiO and  $\text{NiO}_2$ . The nickel dioxide molecule is shown here from nickel and oxygen isotopic shifts and DFT calculations to be linear. The  $(\text{NiO})_2$  rhombic ring exhibits Ni–Ni bonding across the ring with a distance comparable to that in  $\text{Ni}_2$ .

DFT isotopic frequency calculations provide valuable support for vibrational assignments to these nickel oxide and nickel dioxygen species.

Finally, the ONiOO and  $(\text{O}_2)\text{Ni}(\text{O}_2)$  complexes exhibit Fermi resonance which is characterized by both Ni and O isotopic substitution as a measure of mode mixing.

**Acknowledgment.** This work was supported by the Universities of Virginia and Southampton, and this report was taken in part from the M. Chem. thesis of A. Citra, University of Southampton, 1996.

## References and Notes

- (1) Andrews, L.; Chertihin, G. V.; Ricca, A.; Bauschlicher, C. W., Jr. *J. Am. Chem. Soc.* **1996**, *118*, 467.
- (2) Chertihin, G. V.; Saffel, W.; Yustein, J. T.; Andrews, L.; Neurock, M.; Ricca, A.; Bauschlicher, C. W., Jr. *J. Phys. Chem.* **1996**, *100*, 5261–5273.
- (3) Kang, H.; Beauchamp, J. L. *J. Phys. Chem.* **1985**, *89*, 3364.
- (4) Van Zee, R. J.; Hamrick, Y. M.; Weltner, W., Jr. *J. Phys. Chem.* **1992**, *96*, 7247.
- (5) Green, D. W.; Reedy, G. T.; Kay, J. G. *J. Mol. Spectrosc.* **1979**, *78*, 257.

- (6) Srdanov, V. I.; Harris, D. O. *J. Chem. Phys.* **1988**, *89*, 2748
- (7) Ram, R. S.; Bernath, P. F. *J. Mol. Spectrosc.* **1992**, *155*, 315.
- Namiki, K.; Saito, S. *Chem. Phys. Lett.* **1996**, *252*, 343.
- (8) Walch, S. P.; Goddard, W. A., III *J. Am. Chem. Soc.* **1978**, *100*, 1338.
- (9) Panas, J.; Schule, J.; Brademark, U.; Siegbahn, P.; Wahlgren, U. *J. Phys. Chem.* **1988**, *92*, 3079.
- (10) Bauschlicher, C. W., Jr.; Maitze, P. *Theor. Chim. Acta* **1995**, *90*, 1989.
- (11) Huber, H.; Ozin, G. A. *Can. J. Chem.* **1972**, *50*, 3746. Huber, H.; Klotzbucher, W.; Ozin, G. A.; Vander Voet, A. *Can. J. Chem.* **1973**, *51*, 2722.
- (12) Huber, H.; Kundig, E. P.; Moskovits, M.; Ozin, G. A. *J. Am. Chem. Soc.* **1973**, *95*, 332.
- (13) Ozin, G. A.; Klotzbucher, W. E. *J. Am. Chem. Soc.* **1975**, *97*, 3965.
- (14) Andrews, L.; Chertihin, G. V.; Citra, A.; Neurock, M. *J. Phys. Chem.* **1996**, *100*, 11235.
- (15) DGAUSS, UniChem 2.3, Cray Research Inc., Mendota Heights, MN.
- (16) Andzelm, J.; Wimmer, E. *J. Chem. Phys.* **1991**, *96*, 1280.
- (17) Vosko, S. H.; Wilk, L.; Nusair, M. *Can. J. Phys.* **1980**, *58*, 1200.
- (18) Becke, A. D. *Phys. Rev. A* **1988**, *38*, 3098.
- (19) Becke, A. D. *J. Chem. Phys.* **1988**, *88*, 2537.
- (20) Perdew, J. P. *Phys. Rev. B* **1986**, *33*, 8822.
- (21) Godbout, N.; Salahub, D. R.; Andzelm, J.; Wimmer, E. *Can. J. Chem.* **1992**, *70*, 560.
- (22) Huber, K. P.; Herzberg, G. *Constants of Diatomic Molecules*, Van Nostrand Reinhold: New York, 1979.
- (23) Serebrennikov, L. V.; Maltsev, A. A. *Vestn. Mosk. Univ. Ser. 2, Khim.* **1985**, *26*, 464.
- (24) (a) Bondybey, V. E.; English, J. H. *J. Phys. Chem.* **1984**, *88*, 2247. (b) Wu, H.; Desai, S. R.; Wang, L. S. *J. Chem. Phys.* **1995**, *103*, 4363. (c) Chertihin, G. V.; Andrews, L.; Bauschlicher, C. W., Jr. *J. Phys. Chem.*, in press.
- (25) Andrews, L.; Yustein, J. T.; Thompson, C. A.; Hunt, R. D. *J. Phys. Chem.* **1994**, *98*, 6514. Andrews, L.; Chertihin, G. V.; Thompson, C. A.; Dillon, J.; Byrne, S.; Davy, R. D.; Bauschlicher, C. W., Jr. *J. Phys. Chem.* **1996**, *100*, 10088.
- (26) Chertihin, G. V.; Andrews, L. *J. Phys. Chem.* **1995**, *99*, 6356.
- (27) Note that the DFT calculations predict the reverse order for the O—O stretching modes in (O<sub>2</sub>)NiO and (O<sub>2</sub>)NiO<sub>2</sub>, but the N<sub>2</sub>O experiment is definitive in that NiO and the former are produced in high yield, but not ONiO and the latter. Note also that the order of O—O stretching modes assigned to (O<sub>2</sub>)FeO and (O<sub>2</sub>)FeO<sub>2</sub> is opposite those for the Ni species; it is possible that the Fe species assignments should be reversed. The 660.6 cm<sup>-1</sup> iron oxide band is reassigned to the B<sub>2u</sub> mode of (FeO)<sub>2</sub>.
- (28) Moskovits, M.; Hulse, J. E. *J. Chem. Phys.* **1980**, *72*, 2267.
- (29) Anderson, A. B. *J. Chem. Phys.* **1977**, *66*, 5108.
- (30) Morse, M. D.; Hansen, G. P.; Langridge-Smith, P. R. R.; Zheng, L.-S.; Geusic, M. E.; Michalopoulos, D. L.; Smalley, R. E. *J. Chem. Phys.* **1984**, *80*, 5400 and references therein.
- (31) Chertihin, G. V.; Citra, A.; Andrews, L.; Bauschlicher, C. W., Jr., to be published.
- (32) Besenbacher, F.; Norskov, J. K. *Prog. Surf. Sci.* **1993**, *44*, 5.
- (33) Avery, N. R. *Chem. Phys. Lett.* **1983**, *96*, 371.